T. Lang, M. A. Odnoblyudov, V. E. Bougrov, S. Suihkonen, M. Sopanen, H. Lipsanen, Morphology optimization of MOCVD-grown GaN nucleation layers by the multistep technique, Journal of Crystal Growth 292 (2006) 26.

© 2006 Elsevier Science

Reprinted with permission from Elsevier.

Available online at www.sciencedirect.com
SCIENCE DIRECT®
ELSEVIER
Journal of Crystal Growth 292 (2006) 26–32
JOURNAL OF CRYSTAL GROWTH
www.elsevier.com/locate/jcrysgro

Morphology optimization of MOCVD-grown GaN nucleation layers by the multistep technique

T. Lang[a,*], M. Odnoblyudov[b], V. Bougrov[b], S. Suihkonen[a], M. Sopanen[a], H. Lipsanen[a]

[a]*Optoelectronics Laboratory, Micronova Research Center, Helsinki University of Technology, P.O. Box 3500, FIN-02150 HUT, Espoo, Finland*
[b]*Abraham Ioffe Physico-Technical Institute, Politekhnicheskaya 26, 194021 St. Petersburg, Russian Federation*

Received 14 November 2005; received in revised form 20 March 2006; accepted 3 April 2006
Communicated by R.M. Biefeld

Abstract

The heteroepitaxial growth of gallium nitride (GaN) on sapphire substrates by metal-organic chemical vapor deposition is most commonly carried out using the two-step growth process. This process involves the deposition of a thin GaN nucleation layer (NL) at a temperature of approximately 450–600 °C. The morphology of this low-temperature film after annealing is known to have a crucial effect on the quality of GaN buffer layers. In this paper, we report on efficient control of the GaN NL morphology using a multistep technique. The technique is used to control the size and reduce the density of nucleation islands (NIs) on the NL in order to optimize the surface morphology for a subsequent higher temperature overgrowth step. Together with process parameter optimization a density as low as $1\times10^{7}\,\mathrm{cm}^{-2}$ for the NIs is obtained. The NL morphology is analyzed by atomic force microscopy. The dislocation density of GaN buffer layers grown on multistep NLs is evaluated by etch-pit density measurements and X-ray diffraction is used to support and elaborate the results. The crystalline quality of individual NIs is studied by transmission electron microscopy. Measurements indicate that the multistep technique is successfully used to significantly reduce the threading dislocation density in GaN films. A threading dislocation density of $1.0\times10^{8}\,\mathrm{cm}^{-2}$ is demonstrated with the method.

© 2006 Elsevier B.V. All rights reserved.

PACS: 81.15.Gh; 68.55.−a

Keywords: A1. Atomic force microscopy; A1. Etch-pit density; A1. Nucleation; A1. Recrystallization; A3. MOCVD; B1. GaN

1. Introduction

With the demonstration of bright-blue light-emitting diodes (LEDs) and blue laser diodes (LDs) [1–3], III–V nitride semiconductors have emerged as an important material system for high-temperature and high-power optoelectronic applications. One of the biggest problems in the way to developing high-quality nitride-based devices is the lack of suitable substrate materials. III–V nitride structures are most commonly grown on hexagonal (0 0 0 1)-oriented Al_2O_3 (sapphire), which has an approximately 15% smaller in-plane lattice constant than hexagonal gallium nitride (GaN). This large lattice mismatch leads to the formation of a high density of misfit- and threading dislocations (TDs) at the sapphire interface and in the more crucial device layers, respectively. Although commercial quality GaN-based optoelectronic devices are already available, TDs are known to cause degradation in device performance [4,5].

In order to improve material quality and reduce the TD density, a so-called two-step method [6] is often utilized for growing a GaN buffer layer by metal-organic chemical vapor deposition (MOCVD). This method involves the deposition of a thin GaN nucleation layer (NL) at a lower temperature (LT) followed by a high-temperature (HT) growth phase. Upon transition from LT to HT the disordered GaN NL partly decomposes [7]. A material redistribution process [8] leading to the formation of GaN islands accompanies the decomposition. During this

---

[*] Corresponding author.
E-mail address: teemu.lang@hut.fi (T. Lang).

0022-0248/$ - see front matter © 2006 Elsevier B.V. All rights reserved.
doi:10.1016/j.jcrysgro.2006.04.095

redistribution process the surface morphology of the disordered LT GaN film significantly roughens, as material concentrates into islands with a predominantly hexagonal crystalline structure [8,9]. After HT exposure and the associated recrystallization process, the NL contains a large density of Shockley and Frank partial dislocations [9]. On top of the highly faulted HT NL, the large predominantly hexagonal islands contain only few screw- or mixed-type TDs. Most of the TDs are generated during the HT growth stage of the two-step process as the large GaN islands overgrow the HT NL and coalesce. TDs are formed at the coalescence boundaries of adjacent islands, henceforth referred to as nucleation islands (NIs), to accommodate for their relative crystalline misorientation [9].

A significant amount of research has been done to address the issue of TD generation by reducing the density of the NIs on the HT NL. The widely used epitaxial lateral overgrowth (ELOG) has been a successful method in reducing the TD density but the method is very time consuming and expensive as it involves ex-situ masking and patterning of films. Also, in-situ SiN_x micromasking of the sapphire substrate has been used with good results in reducing NI- and TD density and in increasing the average GaN grain size [10–12]. The drawback in this technique, however, is the unintentional n-type doping of GaN caused by Si impurities.

In Ref. [13] we introduced a multistep MOCVD method for growing GaN islands on sapphire. The technique was used to selectively control the size of NIs without affecting their density. Here we report on the significant reduction of NI density utilizing the developed multistep method and process parameter optimization. Additionally, the method is used to grow GaN layers with an ultralow dislocation density on sapphire. Neither in- nor ex-situ masking was needed to obtain the results.

2. Experimental procedure

Each of the studied GaN films were grown in a vertical flow $3 \times 2''$ close-coupled showerhead MOCVD reactor. The precursors used for gallium and nitrogen were TMGa and NH_3, respectively. Hydrogen was used as carrier gas throughout every growth run. The substrates were $2''$ *c*-plane epi-ready sapphire wafers. Before deposition, the substrates went through in-situ annealing at 1070 °C for 300 s in a hydrogen atmosphere. Subsequent surface nitridation was carried out at 530 °C with an ammonia flow of 2 slm for 300 s.

The multistep method was used to grow GaN NLs with a varying number of cycles and with different deposition times for one cycle. One process cycle consisted of first depositing LT GaN at 530 °C and subsequently annealing this film for recrystallization as described in Ref. [13]. After the last annealing step in the growth process, each sample was cooled down to room temperature in an ammonia–hydrogen atmosphere. A TMGa molar flow rate of 60 μmol/min and an ammonia flow of 2 slm, giving a V/III ratio of 1500, were used during the LT deposition steps. During each step of a process cycle, the total pressure was kept constant at 500 Torr. The surface morphology of the NLs was characterized with a NanoScope IIE atomic force microscope (AFM).

In addition to studying the reduction of NI density on a GaN NL by the multistep method, several NLs with a reduced NI density were overgrown with HT GaN. Specifically the effect of total pressure and hydrogen flow on the formation of new islands during the beginning of HT growth was studied. The NLs were overgrown for 300–700 s in a pressure of 200–500 Torr and a hydrogen flow of 10–12 slm. The TMGa molar flow rate was 200 μmol/min and the ammonia flow was 3 slm during the HT overgrowth. The density of newly formed islands in between the NIs was measured with AFM and the crystalline quality and TD density of an individual NI was evaluated by transmission electron microscopy (TEM).

Finally, a comparison was made between the TD densities of GaN films grown on a standard "one-cycle" NL and on a NL optimized with the multistep method. The process parameters of both growth runs were identical after the NL growth. Therefore the differences in the quality of the films can be attributed to the difference in the NL. The TD densities were assessed by etch-pit density (EPD) measurements and high-resolution X-ray diffraction (HR-XRD) was used to support the results.

3. Results and discussion

Many of the crystal growth techniques for low TD GaN buffer layers employ in- or ex-situ masking techniques to reduce the NI density. Previously presented MOCVD growth models for GaN motivate the masking during the initial stages of growth. The models suggest a strong correlation of TD density with the NI density. Moran et al. [14] and Hashimoto et al. [15] have proved this correlation experimentally. In Ref. [15], it is also reported that shorter deposition times for the LT NL results in reduced NI density after HT treatment and recrystallization of the LT layer. The multistep method takes advantage of this phenomenon as it can be used to increase the size of NIs without affecting their density. This enables us to deposit very thin LT NLs and to further reduce the NI density while keeping the size of NIs sufficiently large for them to efficiently act as nucleation centers during HT overgrowth of the NL.

The surface morphology of four GaN NLs is presented in the AFM micrographs of Fig. 1. The NL in Fig. 1(a) (sample A) was prepared with the standard "one-cycle" method by depositing approximately 50 nm of LT film at 530 °C and subsequently up-ramping the temperature to 1060 °C for recrystallization. After this the temperature was ramped down back to 530 °C again. The growth process for samples in Fig. 1(b–d) (samples B, C and D, respectively) consisted of two, three and four process

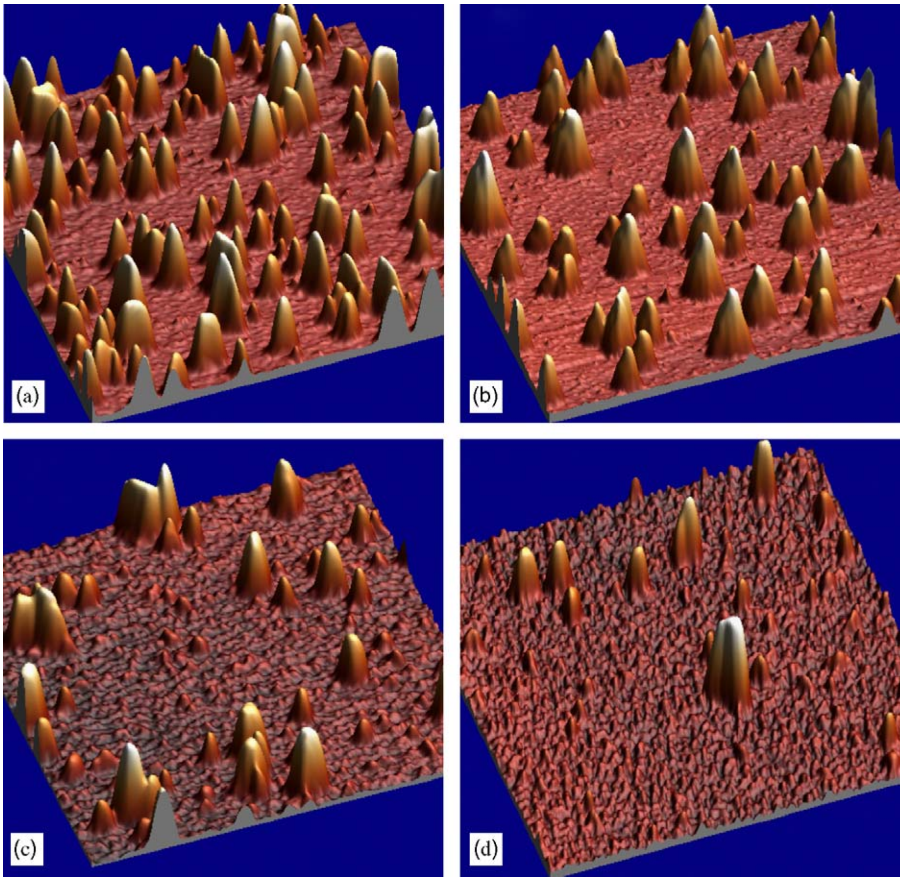

Fig. 1. AFM data illustrating the NI density for (a) sample A, (b) sample B, (c) sample C and (d) sample D. All scans are 10 μm × 10 μm. The height of the largest NIs is about 400 nm in each figure.

cycles, respectively. The total nominal thickness of deposited material was approximately 50 nm for each of the three samples. Thus, the thickness of the LT film deposited in each cycle of the multistep process was 25, 17 and 13 nm for samples B, C and D, respectively. The annealing steps were identical to the one used during the growth of sample A. The presented AFM data indicates a substantial decrease in the NI density. The NI density for the samples A, B, C and D as calculated from Fig. 1 were 1.1×10^8, 7.4×10^7, 4.5×10^7 and $1.7 \times 10^7\,\text{cm}^{-2}$, respectively. Previously SiN_x in-situ micromasking techniques have resulted in NI densities of over $10^8\,\text{cm}^{-2}$ [11].

The reason behind the drastic reduction in NI density is most likely related to the diffusion mechanisms governing the material redistribution process during an annealing step. It has been suggested that the substantial mass transport responsible for the islanding could be explained by the formation of either weaker N–Ga bonds between partially dehydrogenated NH_3 molecules and the GaN surface [16] or by the migration of Ga–N molecules on a Ga-terminated surface [17]. Given that the diffusion lengths and lifetimes of the intermediate species can be extremely large [16], we believe that surface diffusion is not the limiting factor in decreasing the NI density. Rather, a gas-phase diffusion process determines the density of nucleation sites during recrystallization. This argument is supported by previous studies [18] indicating that in addition to decomposition and subsequent surface diffusion, Ga reincorporation through the gas phase into the GaN islands is responsible for their formation. A symptom of this mass transport process is that hexagonal caps are formed on top of disordered phase material during the formation of the NIs as reported in Refs. [8,19]. When the thickness of the LT GaN film deposited before an annealing step decreases so does the volume of material decomposing during annealing. Subsequently the amount of material reincorporated to the film through gas phase becomes smaller resulting in fewer nucleation sites on the NL and consequently to smaller NI densities.

The nominal thickness of material contained in the NIs was 32, 39, 11 and 3 nm for samples A, B, C and D, respectively. Based on our previous study [13] and on the TEM data of the inset of Fig. 3, the nominal NL thickness in between the islands can be assumed to be roughly equal, about 15–30 nm, in each sample. This result suggests that a significant amount of material is lost due to desorption in samples C and D. This type of material loss does not occur when thicker LT GaN films are recrystallized [8,13] since more nucleation sites are available for molecules diffusing on the film surface. Assuming that the diffusing molecules have a limited residence time on the film surface their probability of desorption increases with increasing diffusion distance.

Although we have demonstrated significant reduction in NI density using the multistep NL method, one should also be able to control the overgrowth of the NL in order to prevent new islands from forming during the HT growth phase. Keeping this in mind we have studied the effect of carrier gas flow rate and total reactor pressure on the evolution of film morphology during the initial stages of HT NL overgrowth. The AFM data in Fig. 2(a–d) illustrate the surface morphology for samples E, F, G and H, respectively. The growth process for these samples consisted of first growing a NL with a reduced NI density, similar to sample D (Fig. 1(d)). This NL was subsequently overgrown at HT for 300 s in samples E, F, G and for 700 s in sample H. The total hydrogen flow rate and reactor pressure were 10.5 slm and 200 Torr for sample E, 10.5 slm and 400 Torr for sample F and 12 slm and 500 Torr for both samples G and H. The HT overgrowth temperature was 1060 °C for each sample.

Fig. 2 (a) and (b) clearly indicates how the increase in reactor pressure reduces nucleation in between the sparse NIs obtained by the multistep process (Fig. 1(d)). The GaN island density of about $3.0\times10^{7}\,\mathrm{cm}^{-2}$ in sample F is still substantially higher than the original NI density in sample D. Increasing the total pressure and carrier gas flow rate up to 500 Torr and 12 slm, respectively, further reduces nucleation in between the original NIs. This can be observed from sample G (Fig. 2(c)), where the island density is about $1.7\times10^{7}\,\mathrm{cm}^{-2}$ corresponding to the original NI density in sample D. As the NL overgrowth is continued for 700 s it can be observed that the island density remains constant (Fig. 2(d)) at $1.7\times10^{7}\,\mathrm{cm}^{-2}$ and the growth occurs selectively on the largest islands.

It has been previously reported that increasing reactor pressure enhances GaN decomposition in a H_2 atmosphere [20]. The phenomenon has been exploited in the work of Chen et al. [21] who reported a decrease in the size of nucleation sites (this should not be misinterpreted as a reduction in NI density) as process pressure was increased for the growth of a LT GaN NL. We suggest that the improved nucleation selectivity at higher pressures during the overgrowth of NLs with an extremely low NI density is caused by faster decomposition of the thermally more unstable film in between the NIs. The suppression of nucleation in between the NIs can be further improved by increasing the H_2-carrier gas flow as we have done for samples G and H. This will potentially increase the amount of reactive hydrogen on the film surface required for the GaN decomposition reaction forming NH_3 [20].

A cross-sectional TEM image in Fig. 3 from one of the large islands in sample H indicates that the islands are

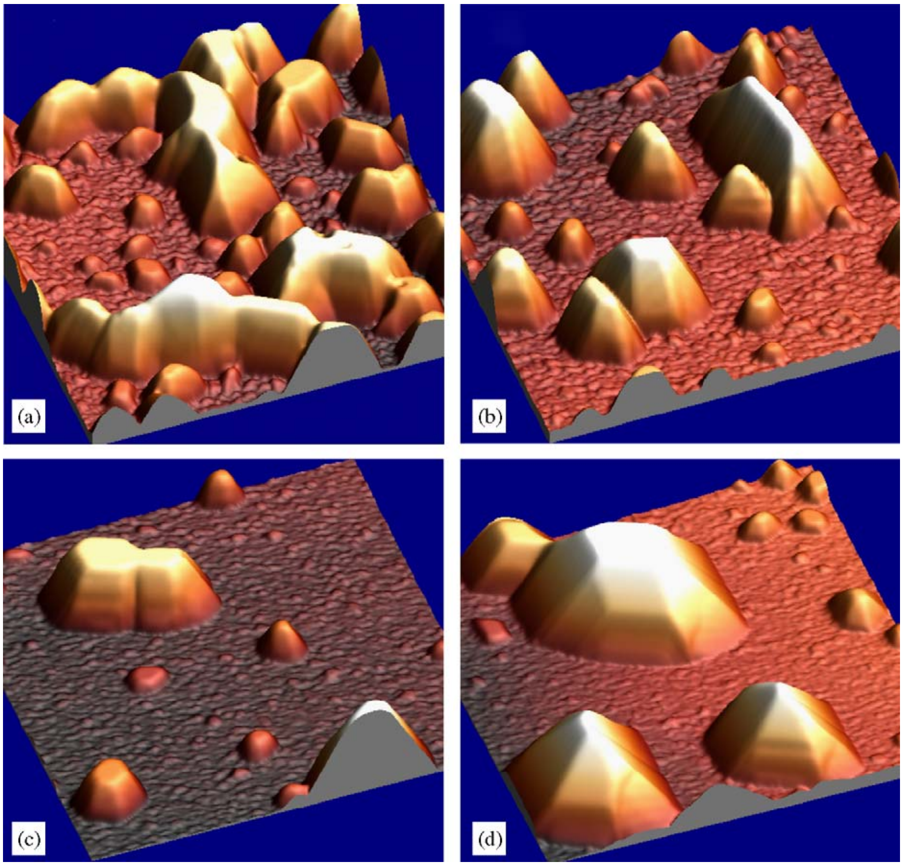

Fig. 2. AFM data illustrating nucleation in between the NIs in the beginning of HT growth. The scans were performed for (a) sample E, (b) sample F, (c) sample G and (d) sample H. All images are 10 μm × 10 μm. The height of the largest islands is about 1 μm in (a–c) and about 1.5 μm in (d).

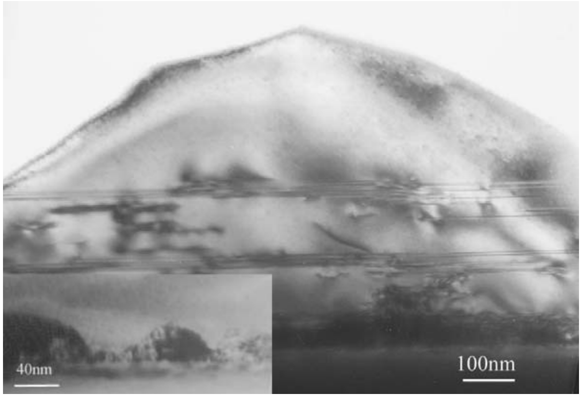

Fig. 3. Cross-sectional TEM micrographs from sample H. In-plane misfit dislocations are clearly visible in the large NI but no TDs penetrating to the surface of the island can be observed. The diffraction conditions for two mutually perpendicular crystalline planes [0 0 0 2] and [0 1 $\bar{1}$ 0] were fulfilled, which allows resolving screw-, edge- and mixed-type dislocations. The NL thickness in between the large NIs can be assessed from the inset illustrating the thin deposit in between NIs in sample H.

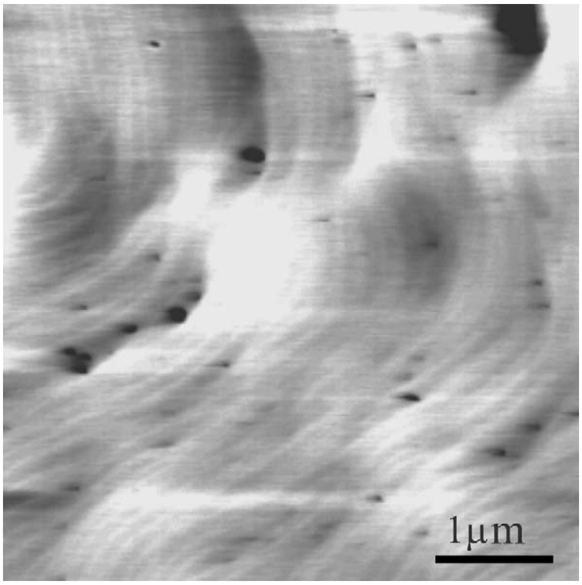

Fig. 4. AFM data illustrating the wavy and pitted surface of a 4.5 μm-thick GaN film. The film was grown on a NL corresponding to sample D with a very sparse distribution of NIs. The scanned area is 5 μm × 5 μm.

essentially free of TDs. This result is in accordance with the previously reported models for GaN growth and TD generation. The image shows that the NI density remains low in sample H during HT overgrowth and small islands are not just merged to form bigger ones. If this were the case more TDs were likely to form inside an island at the coalescence boundaries of smaller islands. A few in-plane misfit dislocations can be observed from the TEM data. These defects may form at the interfaces of regions of different crystalline structure in the island [8].

The ability to reduce NI density and control the unwanted nucleation of GaN in between the NIs during HT overgrowth should theoretically enable the fabrication of GaN films with a lower TD density. GaN buffer layers were grown to evaluate the ability of the multistep NL technique to reduce the number of TDs. The growth process for each sample was identical after completion of the NL, i.e., after the last recrystallization phase. When using NLs such as in samples C and D the NI density was so small that it led to extremely long coalescence times and large island sizes during the overgrowth phase as indicated by Fig. 2(d). The rough surface at this point of the growth process was most likely the reason why pits were observed on top of the GaN buffer layers when too low NI densities (below $5 \times 10^{7}\,\mathrm{cm}^{-2}$) were used. The pits can be seen in the AFM data of Fig. 4 illustrating the as-deposited surface morphology of a 4.5 μm-thick GaN film in which a NL corresponding to sample D was used. Additionally the surface of the sample was wavy indicating an uneven starting surface for the two-dimensional growth phase.

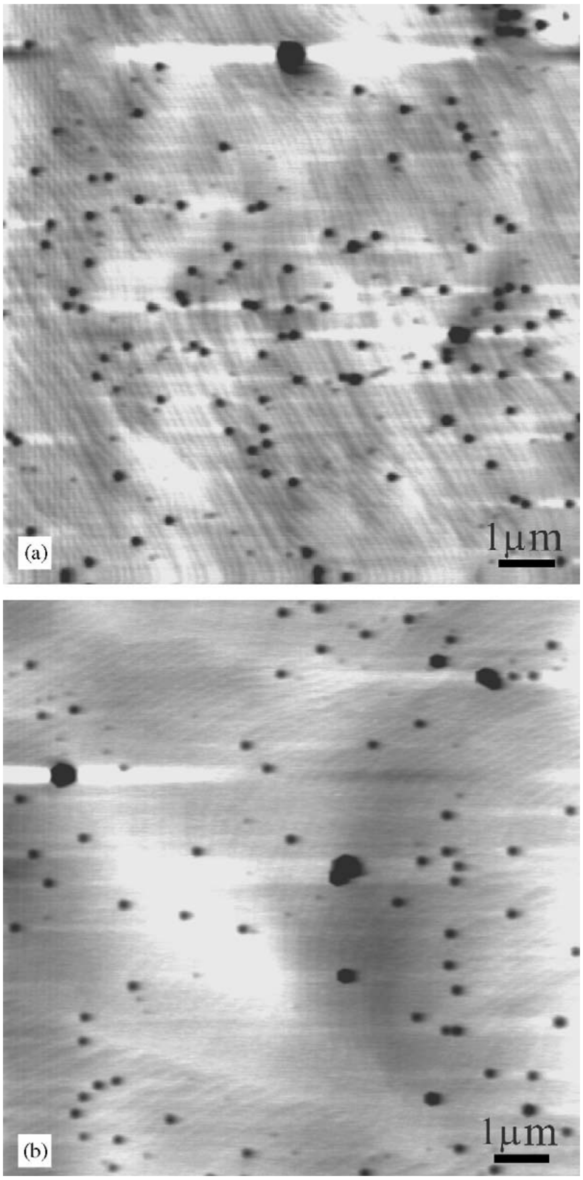

Fig. 5. AFM data illustrating the EPD of GaN films on a standard NL (a) and on a multistep NL (b). Both scans are 10 μm × 10 μm.

The overgrowth stage for the studied GaN buffer layers was optimized for reduced TD density [22]. To evaluate the TD density the samples were etched in a mixture of orthophosphoric and sulfuric acids after the growth process. The density of etch-pits was then measured by AFM. Fig. 5 illustrates the AFM data from two 2.3 μm thick GaN films with etch-pits on their surface. Fig. 5(a) shows the EPD of sample I grown by the standard two-step method. Fig. 5(b) is an EPD scan from sample J in which the multistep technique was used to grow the NL similar to sample B. The calculated EPD was 2.0×10^8 and $1.0 \times 10^8\,\mathrm{cm}^{-2}$ for samples I and J, respectively. By comparing this result with the NI density for samples A and B we observe that the EPD and therefore the TD density decrease roughly in proportion with the NI density of the NL.

Fig. 6 presents XRD data measured from the samples in Fig. 5. The data were obtained from the asymmetric (3 0 2) diffraction. Rocking curve (ω scan) and $2\theta-\omega$ data were recorded for both the samples. These scans indicate a clear improvement in the crystalline quality for the multistep sample. The rocking curve FWHM peak widths in Fig. 6(a) are 363 and 251 arcsec for the standard and the multistep sample, respectively. The result suggests that the TD content is significantly reduced in the GaN film due to the multistep NL [23]. Furthermore, according to the Scherrer formula [24] the coherence lengths in a crystal can be estimated from the peak widths of a $2\theta-\omega$ scan. The FWHM of these peaks is inversely proportional to the coherence length. The 155 and 113 arcsec peak widths in the $2\theta-\omega$ scan data of Fig. 6(b) correspond to a 37% increase in coherence length for the multistep sample. In light of our previously reported results about the reduction in NI density by the multistep technique the increase in coherence length is expected; smaller NI density leads to larger grains (Fig. 2(d)) and increased coherence in the film.

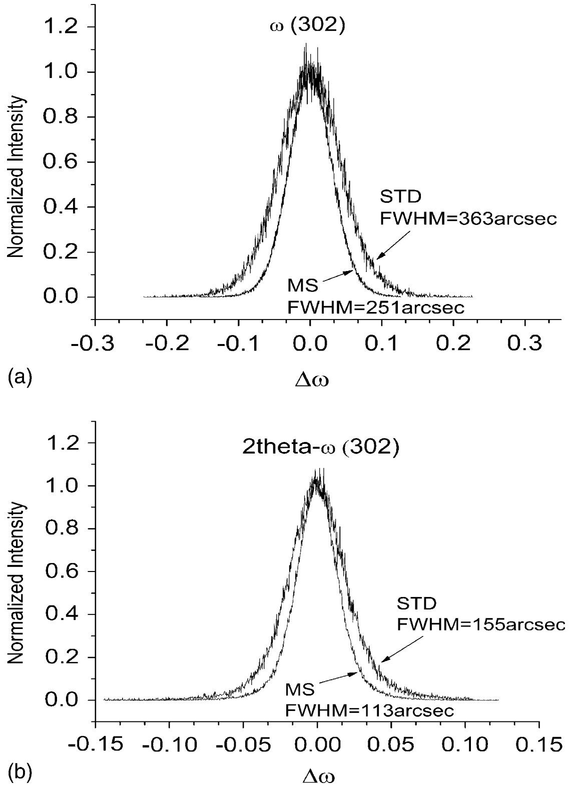

Fig. 6. XRD data from (a) a rocking curve and (b) a $2\theta-\omega$ scan over the (3 0 2)-diffraction peak. Both images illustrate a comparison between GaN layers grown on a standard NL (STD) and on a multistep NL (MS).

4. Conclusions

The multistep method for the MOCVD growth of GaN nucleation layers (NLs) has been studied. The method was used to optimize the surface morphology of a GaN film prior to the high-temperature (HT) coalescence stage of the growth process. By reducing the amount of low-temperature (LT) material deposited in each cycle of the multistep process a drastic decrease in the NI density was obtained. Process parameter optimization was used to suppress GaN growth in between the nucleation islands (NIs) during the beginning of the HT stage. Specifically, it was observed that reactor pressure and hydrogen flow could be used to control the formation of new islands in between the original NIs obtained by the multistep growth. This result was further supported by transmission electron microscopy measurements indicating that no threading dislocations (TDs) are generated inside the NIs during the HT coalescence process.

The effect of the multistep NL method on the TD density of GaN films was studied by measuring etch-pit density with atomic force microscopy (AFM). Rocking curve and 2θ–ω X-ray diffraction scans were performed to support the AFM measurements. Both measurement techniques indicated a significant reduction in the TD density when a multistep NL was used instead of a standard two-step process. An increase in film coherence was also observed in the films grown by the multistep NL method.

Finally, it was observed that with very low NI densities the multistep method resulted in pitting on the buffer layer surface and a wavy surface morphology. This was caused by very large NI size and an extremely rough surface preceding the transition to two-dimensional growth mode. Although the multistep method was successfully used for TD reduction, further improvement in the film quality and surface morphology requires optimization of the overgrowth procedure to enable full coalescence of extremely sparse and large NIs.

Acknowledgments

Financial support by the Finnish Technology Agency (TEKES) and OptoGaN Oy is acknowledged. Maxim Odnoblyudov and Vladislav Bougrov acknowledge the support by RFBR and Dynasty Foundation.

References

[1] S. Nakamura, T. Mukai, M. Senoh, Appl. Phys. Lett. 64 (1994) 1687.

[2] S. Nakamura, M. Senoh, N. Iwasa, S. Nagahama, Jpn. J. Appl. Phys. 34 (1995) L797.

[3] S. Nakamura, M. Senoh, S. Nagahama, N. Iwasa, T. Yamada, T. Matsushita, H. Kiyoku, Y. Sugimoto, Jpn. J. Appl. Phys. 35 (1996) L74.

[4] S.J. Rosner, E.C. Carr, M.J. Ludowise, G. Girolami, H.I. Erikson, Appl. Phys. Lett. 70 (1997) 420.

[5] S. Nakamura, M. Senoh, S. Nagahama, N. Iwasa, T. Yamada, T. Matsushita, Y. Sugimoto, H. Kiyoku, Jpn. J. Appl. Phys. 36 (1997) L1059.

[6] I. Akasaki, H. Amano, Y. Koide, K. Hiramatsu, N. Sawaki, J. Crystal Growth 98 (1989) 209.

[7] D.D. Koleske, M.E. Coltrin, A.A. Allerman, K.C. Cross, C.C. Mitchell, J.J. Figiel, Appl. Phys. Lett. 82 (2003) 1170.

[8] M. Lada, A.G. Cullis, P.J. Parbrook, J. Crystal Growth 258 (2003) 89.

[9] X.H. Wu, P. Fini, E.J. Tarsa, B. Heying, S. Keller, U.K. Mishra, S.P. DenBaars, J.S. Speck, J. Crystal Growth 189/190 (1998) 231.

[10] S. Haffouz, H. Lahreche, P. Vennegues, P. de Mierry, B. Beaumont, F. Omnes, P. Gibart, Appl. Phys. Lett. 73 (1998) 1278.

[11] E. Frayssinet, B. Beaumont, J.P. Faurie, P. Gibart, Z. Makkai, B. Pecz, P. Lefebvre, P. Valvin, MRS Internet J. Nitride Semicond. Res. 7 (2002) 8.

[12] R. Datta, M.J. Kappers, M.E. Vickers, J.S. Barnard, C.J. Humphreys, Superlattices Microstruct. 36 (2004) 393.

[13] T. Lang, M. Odnoblyudov, V. Bougrov, M. Sopanen, J. Crystal Growth 277 (2005) 64.

[14] B. Moran, F. Wu, A.E. Romanov, U.K. Mishra, S.P. DenBaars, J.S. Speck, J. Crystal Growth 273 (2004) 38.

[15] T. Hashimoto, M. Yuri, M. Ishida, Y. Terakoshi, O. Imafuji, T. Sugino, K. Itoh, Jpn. J. Appl. Phys. 38 (1999) 6605.

[16] D.D. Koleske, A.E. Wickenden, R.L. Henry, W.J. DeSisto, R.J. Gorman, J. Appl. Phys. 84 (1998) 1998.

[17] H. Liu, J.G. Kim, M.H. Ludwig, R.M. Park, Appl. Phys. Lett. 71 (1997) 347.

[18] D.D. Koleske, M.E. Coltrin, K.C. Cross, C.C. Mitchell, A.A. Allerman, J. Crystal Growth 273 (2004) 86.

[19] K. Lorenz, M. Gonsalves, W. Kim, V. Narayanan, S. Mahajan, Appl. Phys. Lett. 77 (2000) 3391.

[20] D.D. Koleske, A.E. Wickenden, R.L. Henry, J.C. Culbertson, M.E. Twigg, J. Crystal Growth 223 (2001) 466.

[21] J. Chen, S.M. Zhang, B.S. Zhang, J.J. Zhu, G. Feng, X.M. Shen, Y.T. Wang, H. Yang, W.C. Zheng, J. Crystal Growth 254 (2003) 348.

[22] S. Kim, J. Oh, J. Kang, D. Kim, J. Won, J. Kim, H. Cho, J. Crystal Growth 262 (2004) 7.

[23] B. Heying, X.H. Wu, S. Keller, Y. Li, D. Kapolnek, B.P. Keller, S.P. DenBaars, J.S. Speck, Appl. Phys. Lett. 68 (1996) 643.

[24] P. Fewster, X-ray Scattering from Semiconductors, Imperial College Press, London, 2000.